Developmental Cell
Article

BCL6 Canalizes Notch-Dependent Transcription, Excluding Mastermind-like1 from Selected Target Genes during Left-Right Patterning

Daisuke Sakano,[1] Akiko Kato,[1] Nisarg Parikh,[1] Kelly McKnight,[1] Doris Terry,[1] Branko Stefanovic,[1] and Yoichi Kato[1,*]
[1]Department of Biomedical Sciences, Florida State University, College of Medicine, Tallahassee, FL 32306, USA
*Correspondence: yoichi.kato@med.fsu.edu
DOI 10.1016/j.devcel.2009.12.023

SUMMARY

Although the Notch signaling pathway is one of the most intensely studied intracellular signaling pathways, the mechanisms by which Notch signaling regulates transcription remain incompletely understood. Here, we report that B cell leukemia/lymphoma 6 (BCL6), a transcriptional repressor, is a Notch-associated factor. BCL6 is necessary to maintain the expression of *Pitx2* in the left lateral plate mesoderm during the patterning of left-right asymmetry in *Xenopus* embryos. For this process, BCL6 forms a complex with BCL6 corepressor (BCoR) on the promoters of selected Notch target genes such as *enhancer of split related 1*. BCL6 also inhibits the transcription of these genes by competing for the Notch1 intracellular domain, preventing the coactivator Mastermind-like1 (MAM1) from binding. These results define a mechanism restricting Notch-activated transcription to cell-type-appropriate subsets of target genes, and elucidate its relevance in vivo during left-right asymmetric development.

INTRODUCTION

Vertebrates show conserved anatomical left-right (LR) asymmetry of the internal organs such as the orientation of the cardiovascular system, visceral organs, and the number of lung lobes, whereas their external bodies are bilaterally symmetrical (Levin, 2005; Palmer, 2004). Although many of the mechanisms involved in breaking LR symmetry during early development may not be conserved, the universal hallmark of vertebrate LR asymmetric development is left-side-specific expression of genes such as *Nodal*, *Lefty*, and *Pitx2* in the lateral plate mesoderm (LPM) (Boorman and Shimeld, 2002; Raya and Belmonte, 2006; Speder et al., 2007). Indeed, these genes play crucial roles during the patterning of LR asymmetry (Capdevila et al., 2000; Hamada et al., 2002).

The Notch signaling pathway is a well conserved signaling pathway in animals (Borggrefe and Oswald, 2009). After an interaction between the Delta/Serrate/Lag-2 (DSL) ligand and the Notch receptor, the Notch receptor intracellular domain (NICD) is released from the membrane by two sequential proteolytic cleavages. NICD subsequently translocates into the nucleus and forms a complex with nuclear proteins, including the C-promoter-binding factor 1/Suppressor of Hairless/Lag-1 (CSL) transcriptional factor and the transcriptional coactivator, Mastermind-like (MAM), to activate the transcription of target genes. Notch signaling has been demonstrated to affect LR asymmetry in mice (Krebs et al., 2003; Raya et al., 2003), chick (Raya et al., 2004), and zebrafish (Kawakami et al., 2005; Raya et al., 2003). Previous studies in mice demonstrated that Notch signaling directly regulates early symmetric expression of *Nodal* through a node-specific enhancer (Adachi et al., 1999; Brennan et al., 2002; Norris and Robertson, 1999), which contains two functional binding sites for CSL (Krebs et al., 2003; Raya et al., 2003). Interestingly, although the expression of *Pitx2* in the left LPM is initiated by Nodal (Shiratori et al., 2001), it can also be induced by downregulation of Notch signaling even in the absence of Nodal function (Krebs et al., 2003; Raya et al., 2003), suggesting that the expression of *Pitx2* is regulated by both Nodal-dependent and -independent mechanisms. Thus far, the regulatory mechanism governing *Pitx2* expression remains incompletely understood.

B cell leukemia/lymphoma 6 (BCL6) is a sequence-specific transcriptional repressor that recruits a wide variety of corepressors, including BCL6 corepressor (BCoR) (Huynh et al., 2000). BCL6 was originally identified via chromosomal translocations affecting band 3q27, which are common in B cell non-Hodgkin lymphoma (Baron et al., 1993; Kerckaert et al., 1993; Ye et al., 1993). In fact, deregulated *BCL6* expression is commonly observed in diffuse large B cell lymphomas and follicular lymphomas (Ohno, 2004; Pasqualucci et al., 2003). During normal B cell development, BCL6 is required for the formation of germinal centers (GC) (Dent et al., 1997; Ye et al., 1997) and maintains the expression of GC-specific genes by suppressing genes involved in B cell activation in response to DNA damage, cell cycle regulation, and plasma cell differentiation (Li et al., 2005; Niu et al., 2003; Phan and Dalla-Favera, 2004; Ranuncolo et al., 2007; Shaffer et al., 2001; Tunyaplin et al., 2004; Vasanwala et al., 2002). Whereas the function of BCL6 in the formation of lymphoma and normal B cell development has been well studied, its roles during embryogenesis are poorly understood.

Here, we report that BCL6 is a transcriptional repressor associated with Notch signaling during *Xenopus* LR patterning. By binding NICD, preventing MAM1 recruitment, and associating instead with BCoR, BCL6 inhibits certain Notch-induced target genes such as *enhancer of split related 1* (*ESR1*). Target gene specificity is achieved by direct binding of BCL6 to relevant

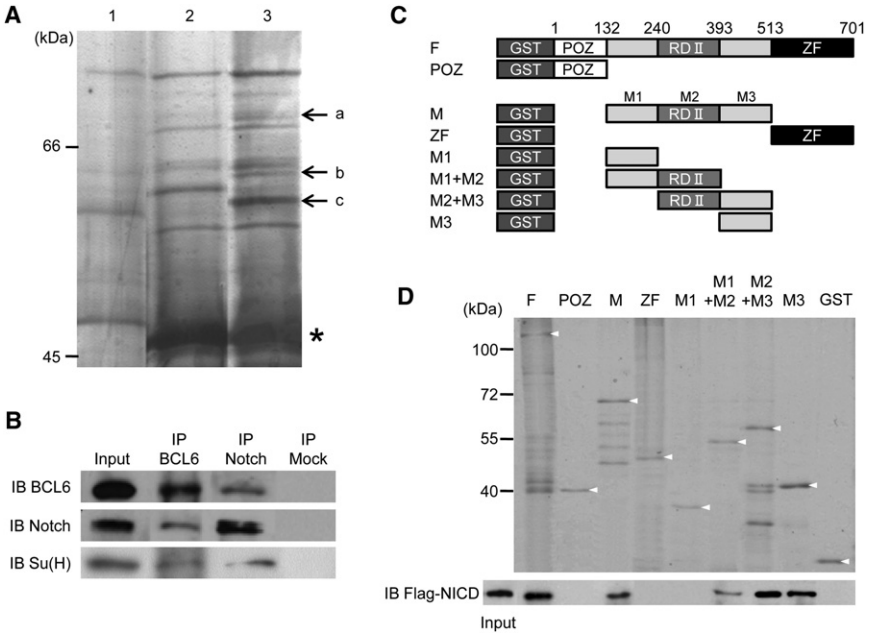

Figure 1. BCL6 Interacts with the ANK Domain of Notch1

(A) Lane 1, GST/embryonic protein extract; lane 2, GST-ANK; and lane 3, GST-ANK/embryonic protein extract. a, BCL6; c, β-actin. GST-ANK is indicated by an asterisk.

(B) Protein extracts from stage-25 embryos were incubated with α-Notch1 or α-BCL6 antibody. Mouse IgG was used for a mock immunoprecipitation.

(C) GST-BCL6 constructs. The numbers on the top indicate the positions of amino acids.

(D) The top panel shows the expression of GST constructs, and the bottom panel shows the interactions between Flag-tagged NICD (Flag-NICD) and GST-BCL6 constructs. Each arrowhead indicates an intact GST fusion protein.

enhancer elements. This function helps maintain the expression of *Pitx2* and thus LR asymmetry. Our studies elucidate crosstalk between Notch signaling and the BCL6/BCoR complex, and further show that BCL6 functions as a repressor of Notch signaling during LR patterning.

RESULTS

Isolation of Notch-Associated Proteins

In studies to understand how Notch signaling regulates transcription during embryogenesis, we sought novel transcriptional regulators that can interact with NICD. A GST fusion protein containing the ankyrin-like repeats domain of NICD protein (GST-ANK) was used to isolate interacting proteins by immunoprecipitation. The ANK domain was utilized because it is an important domain required for the transcriptional activation of Notch signaling and for interaction with the CSL transcriptional factor (Kato et al., 1997), MAM (Kurooka et al., 1998), the histone acetyltransferase complex (Tani et al., 2001), and Deltex (Diederich et al., 1994; Matsuno et al., 1995). Precipitation was performed with GST-ANK and protein extracts from 100 embryos at stages 15, 20, and 25. The coprecipitated proteins were separated by one-dimensional (1D) gel electrophoresis, followed by silver staining (Figure 1A). Three bands in lane 3 (GST-ANK + protein extract) were specific when compared with lane 1 (GST + protein extract), which shows GST-associated bacterial and embryonic proteins, and lane 2 (GST-ANK alone), which shows GST-ANK-associated bacterial proteins. Via mass spectrometry analysis, we identified one of these bands, indicated by "a" in Figure 1A, as BCL6. Deltex1, which is a regulator of Notch signaling (Diederich et al., 1994; Matsuno et al., 1995, 1998), was also identified from the same protein band, although the MASCOT score was not high (data not shown). To determine if BCL6 endogenously interacts with Notch1, we performed coimmunoprecipitation studies with α-Notch antibody, which recognizes the intracellular domain of Notch1, or α-BCL6 antibody. Using protein extracts from *Xenopus* embryos, a specific endogenous association between Notch1 and BCL6 was observed (Figure 1B). In addition, Suppressor of Hairless (Su(H)), a *Xenopus* ortholog of CSL, was also coprecipitated by α-BCL6 antibody (Figure 1B).

To delineate the domain of BCL6 responsible for the interaction with Notch1, binding assays were performed. As the known functional domains of BCL6 are the POZ/BTB domain (POZ) at the N terminus, the repression domain II (RDII) in the middle, and the C2H2-type zinc finger (ZF) domain at the C terminus (Albagli-Curiel, 2003; Chang et al., 1996), eight GST-BCL6 fusion constructs harboring the individual domains were generated (Figure 1C). Immunoprecipitation studies between in vitro-translated Flag-tagged NICD protein and purified GST-fused BCL6 fragments were performed. The Notch-binding domain of BCL6 was localized to the region of BCL6 that harbored the RDII region (M2 in Figure 1C) and the M3 region (Figure 1D). These regions also interacted with the ANK domain alone (see Figure S1A available online). In addition, interaction studies with in vitro-translated proteins demonstrate that BCL6 appears to directly interact with NICD, but not Su(H) (Figure S1B).

BCL6 Is Required for the Patterning of the LR Axis in *Xenopus*

To determine functional roles for BCL6 in Notch signaling, the role of BCL6 during embryogenesis was first examined. *BCL6* was expressed in ectodermal and mesodermal tissues through early embryogenesis (Figures S2A and S2B). The injection of the highest dose (2 ng) of *BCL6* RNA into one blastomere of 2-cell-stage embryos or a single dorsal or ventral blastomere of 4-cell-stage embryos did not elicit any morphological changes in the injected embryos (data not shown). We employed a Morpholino Antisense Oligo (MO) against *BCL6* (BCL6 MO), which binds sequences encompassing the ATG site of directed transcripts and inhibits protein translation, thus depleting the endogenous protein (Heasman et al., 2000). The injection of BCL6 MO significantly reduced endogenous BCL6 protein (Figure S2C). BCL6 MO or a control MO (Control MO), which targets human

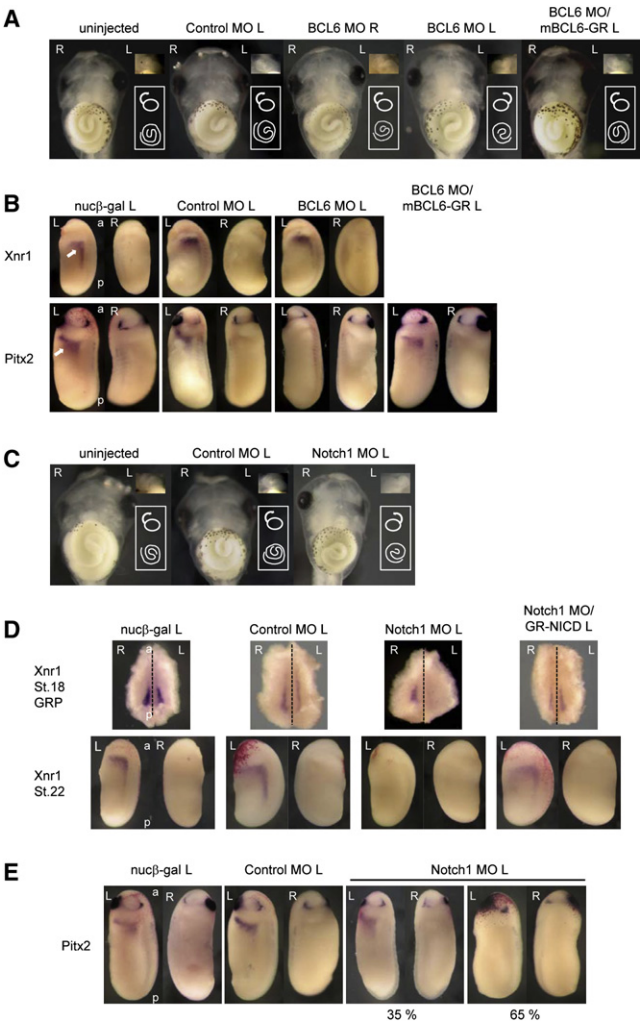

Figure 2. Related Functions of BCL6 and Notch Signaling during LR Patterning

(A) 40 ng BCL6 MO, 40 ng Control MO, or/and 2 ng *mBCL6-GR* was injected for each experiment. An arrow or a spiral indicates the orientation of the heart or the gut coiling, respectively. Ventral views are shown.

(B) The normal left-specific expression of *Xnr1* or *Pitx2* is indicated by an arrow in the *nucβ-gal*-injected embryo.

(C) 80 ng Notch1 MO or 80 ng Control MO was injected for each experiment. An arrow or a spiral indicates the orientation of the heart or the gut coiling, respectively. Ventral views are shown.

(D and E) 150 ng Notch1 MO, 150 ng Control MO, or/and 1 ng *GR-NICD* RNA was injected for each experiment. The dotted line indicates the embryonic midline. The injected side is indicated by "L" (left) or "R" (right) beside the names of the injected samples. L, left; R, right; a, anterior; p, posterior.

beta-globin pre-mRNA and does not recognize *BCL6* mRNA, was injected into a dorsal blastomere of 4-cell-stage embryos. *Green fluorescent protein* (*GFP*) RNA was coinjected as a tracer (data not shown). When 40 ng BCL6 MO was injected into a left dorsal blastomere of 4-cell-stage embryos, striking abnormalities in the orientation of gut origin, gut coiling, and the heart were observed (Figure 2A; Table 1). The gut origin occurred at the left (27.8%, n = 115) and gut coiling was clockwise (34%, n = 115), whereas the normal gut origin occurs at the right and normal gut coiling is counterclockwise. The orientation of the heart was also inverted in a number of these BCL6 MO-injected embryos (24.4%, n = 115). Phenotypes were scored according to Branford et al. (2000). In contrast, there is no significant effect in the Control MO-injected or right-side BCL6 MO-injected embryos. In addition, the defects of gut extension were observed in ~30% of the BCL6 MO-injected embryos, and these embryos were not included when phenotypes were scored (data not shown). To show the specificity of the BCL6 MO effect, we coinjected BCL6 MO and a hormone-inducible mutant *BCL6* (mBCL6-GR) RNA, whose translation initiation site was replaced by the Myc tag and which is no longer recognized by BCL6 MO, and examined gut and heart phenotypes. Except where noted otherwise, we consistently added dexamethasone (DEX) to the medium at stage 20, to activate a GR-fused protein. Thus activated, mBCL6-GR rescued gut origin (27.8% to 4.3%), gut coiling (34% to 7.5%), and the heart (24.4% to 3.3%) phenotypes to normal (Figure 2A; Table 1). As the failure of LR asymmetric patterning causes the disorientation of gut origin, gut coiling, and the heart (Branford et al., 2000), these results suggest that the expression of BCL6 in the left side of embryos is necessary for LR patterning.

To further study the role of BCL6 in the patterning of LR asymmetry, we first characterized the role of BCL6 in the conserved Nodal-Pitx2 cascade that governs LR patterning. The expression of left-side-specific genes, *Xnr1* (a Nodal paralog) and *Pitx2* (Lohr et al., 1997; Ohi and Wright, 2007; Schweickert et al., 2000; Vonica and Brivanlou, 2007), were tested in the BCL6-depleted embryos. BCL6 MO or Control MO was injected into a left dorsal blastomere of 4-cell-stage embryos, and the expression of *Xnr1* at stage 22 and *Pitx2* at stage 25 in the left LPM was examined. Interestingly, the injection of BCL6 MO suppressed the expression of *Pitx2* (100%, n = 28), but not *Xnr1* (0%, n = 28) (Figure 2B; see RT-PCR in Figures S2D and S2E). As with the general embryonic LR defects, these gene expression patterns were also rescued by coinjection of *mBCL6-GR* (0% to 97%) (Figure 2B). Although we were unable to detect *BCL6* in the left LPM at stage 25 by whole-mount in situ hybridization (Figure S2A), RT-PCR clearly revealed LR symmetric *BCL6* expression in the LPM at this stage (Figure S2F). Thus, BCL6 is required for the expression of *Pitx2*, but not *Xnr1*, in the left LPM.

Dual Roles of Notch Signaling during LR Patterning Are Conserved in *Xenopus*

Previous studies in mice showed that Notch signaling initiates the symmetric expression of *Nodal* perinodally, whereas the downregulation of Notch signaling acts independently of Nodal at later stages, to allow the expression of *Pitx2* in the LPM (Krebs et al., 2003; Raya et al., 2003). This suggests that Notch signaling is involved in the regulation of both *Nodal* and *Pitx2* expression at different developmental stages. In particular, Notch activity at the later stage, which could suppress the expression of *Pitx2*, may be a possible target of BCL6 during LR patterning. We therefore sought to confirm that Notch signaling has a conserved function in these aspects of LR patterning in *Xenopus*.

At stage 18, *Xenopus Notch1* and Notch ligands, *Delta1* and *Serrate1*, were expressed on the gastrocoel roof plate (GRP), which is analogous to the amniote node (Schweickert et al., 2007) (Figure S2G); this is where the expression of *Xnr1* is

Table 1. Laterality Scoring in BCL6 MO, NBD-S, or Notch1 MO Injection

		Cardiac Orientation, Forward				Cardiac Orientation, Reverse				
		Gut Origin Right		Gut Origin Left		Gut Origin Right		Gut Origin Left		
Injection	Injection Side	CCW[a]	CW[b]	CCW	CW	CCW	CW	CCW	CW	n
Uninjected		95.4	2.3	0.8	1.5	0.0	0.0	0.0	0.0	130
BCL6 MO										
40 ng Control MO	Left	96.1	1.3	2.6	0.0	0.0	0.0	0.0	0.0	76
20 ng Control MO	Left	97.8	1.1	1.1	0.0	0.0	0.0	0.0	0.0	89
40 ng BCL6 MO	Right	90.5	1.9	1.9	1.0	1.0	0.0	1.9	1.9	105
20 ng BCL6 MO	Right	90.7	1.9	3.7	0.9	0.9	0.0	0.9	0.9	108
40 ng BCL6 MO	Left	47.0	11.3	7.8	9.6	7.0	7.0	4.3	6.1	115
20 ng BCL6 MO	Left	59.5	20.2	6.0	9.5	1.2	2.4	0.0	1.2	84
40 ng BCL6 MO/2 ng mBCL6-GR	Left	89.4	4.3	1.1	2.1	1.1	1.1	1.1	0.0	94
20 ng BCL6 MO/2 ng mBCL6-GR	Left	85.7	3.1	2.0	1.0	1.0	2.0	2.0	3.1	98
NBD-S										
1 ng NBD-S-GR	Left	70.0	7.0	6.0	3.0	5.0	2.0	4.0	3.0	100
2 ng NBD-S-GR	Left	55.0	11.0	9.0	4.0	4.0	3.0	8.0	4.0	98
Notch1 MO										
150 ng Control MO	Left	83.7	2.4	8.1	2.4	0.8	0.8	0.8	0.8	123
80 ng Control MO	Left	91.3	3.6	2.2	2.9	0.0	0.0	0.0	0.0	138
150 ng Notch1 MO	Left	38.7	33.1	8.9	6.5	2.4	4.0	3.2	3.2	124
80 ng Notch1 MO	Left	57.1	22.7	4.2	1.7	3.4	3.4	4.2	3.4	119

Lateral scoring is according to Branford et al. (2000). Numbers indicate the percentage of embryos displaying the phenotype (total embryos as n).
[a] CCW, counterclockwise.
[b] CW, clockwise.

initiated (Jones et al., 1995; Lustig et al., 1996) early during the acquisition of LR asymmetry. *Notch1* and *Serrate1*were also expressed in the LPM at stage 25, similar to *BCL6* (Figure S2F), but *Delta1* was hardly detected by RT-PCR (data not shown). The injection of Notch1 MO significantly reduced endogenous Notch1 protein (Figure S2C) and the expression of Notch target genes (Figure S2H). When 80 ng Notch1 MO or Control MO was injected into a left dorsal blastomere of 4-cell-stage embryos, the orientation of gut origin (13.5%, n = 119), gut coiling (31.2%, n = 119), and heart looping (14.4%, n = 119) was often inverted (Figure 2C; Table 1). And, again, as seen in the BCL6 MO experiments, defects in gut extension were observed in ~25% of the Notch1 MO-injected embryos, and these embryos were not included when phenotypes were scored (data not shown). Unlike BCL6 MO, however, the Notch1 MO suppressed the expression of *Xnr1* on both sides of the GRP at stage 18 (left: 93%, n = 30; right: 89%, n = 28) (Figure 2D; Figure S2I) and in the left LPM at stage 22 (100%, n = 30) (Figure 2D). Although *Xnr1* expression in the GRP was not decreased in all cases, its expression completely disappeared from the LPM at stage 22. The effects of the Notch1 MO were rescued by a hormone-inducible *NICD* (GR-NICD) RNA. When GR-NICD was activated by DEX at stage 12, *Xnr1* expression in the GRP at stage 18 (left: 7% to 92%; right: 11% to 86%) and the left LPM at stage 22 (0% to 60%) was restored to normal levels (Figure 2D; Figure S2I). These data indicate that *Xenopus* Notch signaling promotes the expression of *Xnr1* in the GRP during LR patterning.

The expression of *Pitx2* in the Notch1 MO-injected embryos was next examined. As *Xnr1* expression in the stage-22 LPM was not observed in the Notch1 MO-injected embryos and the expression of *Pitx2* is initiated by Xnr1 (Ohi and Wright, 2007), we predicted that *Pitx2* expression would be completely abolished in the Notch1 MO-injected embryos. However, *Pitx2* expression was affected in only some of these embryos (65%, n = 31) (Figure 2E). Interestingly, when Notch1 MO and *GR-NICD* RNA were coinjected for the rescue study, the expression of *Pitx2* was not rescued, and the number of embryos with suppressed *Pitx2* increased (65% to 100%, data not shown). Accordingly, LR asymmetry defects induced by Notch1 MO were not rescued by coinjection of *GR-NICD* (data not shown). These findings suggest that, as in mice (Krebs et al., 2003; Raya et al., 2003), the expression of *Xenopus Pitx2* could occur when Notch signaling was downregulated in the absence of Xnr1 function, and Notch signaling could suppress the expression of *Pitx2*. We therefore decided to test this hypothesis in more detail.

Indeed, when *GR-NICD* RNA was injected into a left dorsal blastomere of 4-cell-stage embryos and GR-NICD was activated by DEX treatment at stage 20, *Pitx2* expression was suppressed (90%, n = 30) (Figure 3A). However, even when GR-NICD was activated at stage 12, the expression of *Xnr1* remained unchanged (Figure 3A). Although an increase in *Xnr1* expression might have been expected, this result is consistent with the fact that overexpression of GR-NICD on the right side rarely induced the expression of *Xnr1* (6%, n = 32) or *Pitx2* (0%, n = 31) on the injected side (data not shown). It is unclear why NICD is insufficient to induce *Xnr1* or *Pitx2* in *Xenopus*, but is sufficient to do so in zebrafish (Raya et al., 2003); however, it is easy to imagine that other factors required for *Xnr1* expression are not

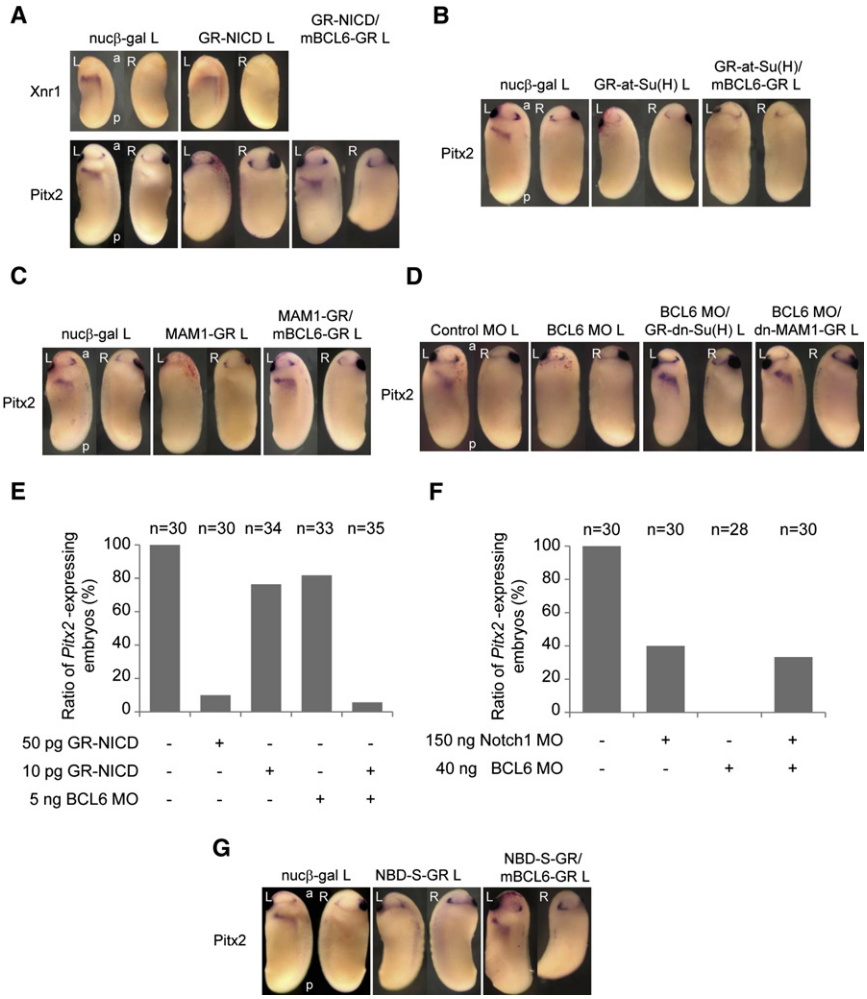

Figure 3. BCL6 Maintains *Pitx2* Expression by Inhibiting Notch Signaling

(A–D) 50 pg *GR-NICD*, 100 pg *GR-at-Su(H)*, 100 pg *MAM1-GR*, 2 ng *GR-dn-Su(H)*, 2 ng *dn-MAM1-GR*, or/and 2 ng *mBCL6-GR* was injected for each experiment.

(E and F) The expression of *Pitx2* at stage 25 was tested by whole-mount in situ hybridization, and the ratios of the *Pitx2*-expressing embryo number versus the total tested embryo number are shown. The total numbers of each injection are shown as "n" on the top of each bar.

(G) 2 ng *NBD-S-GR* or/and *mBCL6-GR* was injected for each experiment. The injected side is indicated by "L" (left) beside the names of the injected samples. L, left; R, right; a, anterior; p, posterior.

adequately expressed on the right side in *Xenopus*, and, conversely, that NICD overexpression in zebrafish may only exert early effects (on Nodal paralog expression), but may not last long enough to inhibit *Pitx2*. In any case, taken together, these findings suggest the possibility that BCL6 selectively antagonizes Notch-mediated inhibition of *Pitx2* expression in *Xenopus*, and that this antagonism forms the basis for BCL6 requirements during LR asymmetric development.

BCL6 Inhibits Notch and Maintains *Pitx2* Expression by Interfering with MAM1

To test the possibility that BCL6 is necessary to suppress Notch activity and maintain *Pitx2* expression, *GR-NICD* and *mBCL6-GR* RNA were coinjected into a left dorsal blastomere of 4-cell-stage embryos, and the expression of *Pitx2* was tested. BCL6 restored the expression of *Pitx2* to normal levels (10% to 58%) (Figure 3A), indicating that Notch signaling is indeed a likely target of BCL6 during LR patterning.

We next examined whether the suppression of *Pitx2* by Notch signaling is mediated by Su(H) or MAM1. A hormone-inducible active type of *Su(H)* fused to the VP16 activator domain (GR-at-Su(H)) (Rones et al., 2000), or a hormone-inducible *MAM1* (MAM1-GR) RNA, was injected into a left dorsal blastomere of 4-cell-stage embryos, and the expression of *Pitx2* was examined. Both at-Su(H) (90%, n = 31) and MAM1 (91%, n = 32) suppressed the expression of *Pitx2* (Figures 3B and 3C). To test whether the suppression of *Pitx2* by Su(H) or MAM1 is inhibited by BCL6, *GR-at-Su(H)* or *MAM1-GR* RNA was coinjected with *mBCL6-GR*. BCL6 rescued MAM1 effects on *Pitx2* (9% to 61%) (Figure 3C), but not at-Su(H) effects on *Pitx2* (10% to 13%) (Figure 3B), suggesting that BCL6 may interfere with specific aspects of transcriptional activation by the NICD/Su(H) complex. As at-Su(H) can activate transcription of Notch target genes without NICD, this result further suggests that BCL6 does not compete with Su(H) to bind to the CSL-binding sites in the promoters of target genes. To confirm the idea that BCL6's principal function in this context is to block Notch-dependent transcription, we used a hormone-inducible dominant-negative form of Su(H) (GR-dn-Su(H)), which has a mutation in the DNA-binding domain and can still interact with NICD (Rones et al., 2000; Wettstein et al., 1997), and a hormone-inducible dominant-negative form of MAM1 (dn-MAM1-GR), which has only the Notch-binding domain (Kiyota and Kinoshita, 2002). Coinjection of *GR-dn-Su(H)* or *dn-MAM1-GR* RNA with BCL6 MO restored *Pitx2* expression to normal levels (8% to 75% with GR-dn-Su(H), n = 24; 8% to 84% with dn-MAM1-GR, n = 25) (Figure 3D), indicating that blocking transcriptional outputs of Notch signaling can rescue BCL6 MO phenotypes.

To further confirm endogenous crosstalk between Notch signaling and BCL6, the following studies were performed. The maximum amounts of *GR-NICD* RNA (10 pg) and BCL6 MO (5 ng), which alone cannot sufficiently suppress the expression of *Pitx2*, showed a synthetic interaction, suppressing *Pitx2* (Figure 3E) and suggesting that endogenous BCL6 inhibits Notch activity. Moreover, the Notch1 MO was epistatic to the BCL6 MO (Figure 3F), indicating that Notch signaling is an in vivo target of BCL6 for the expression of *Pitx2* (Figure S3A).

In order to design a reagent that would selectively block BCL6/Notch interactions, without affecting other BCL6 or Notch functions, a hormone-inducible mutant BCL6 construct (NBD-S-GR), which contains only the M3 domain, was generated (Figure 1C). To our knowledge, the M3 domain has not been reported to be required for the interaction between BCL6 and any other factors thus far, yet we find it is sufficient to interfere with the interaction between Notch1 and BCL6, while leaving the NICD transcriptional complex (Figure S3B) and Notch activity (Figures S3C and S3D) intact. *NBD-S-GR* RNA was injected into the left dorsal blastomere of 4-cell-stage embryos, and the expression of *Pitx2* was examined. The expression of *Pitx2* was inhibited by NBD-S (87%, n = 31), and this inhibition was rescued by the coinjection of *mBCL6-GR* RNA (13% to 76%) (Figure 3G). Note that the defects of LR asymmetry were also observed in the NBD-S-injected embryos (Table 1). To verify whether NBD-S enhances the ability of Notch to suppress *Pitx2*, the maximum amounts of *GR-NICD* (10 pg) and *NBD-S-GR* (100 pg), which alone cannot sufficiently suppress the expression of *Pitx2*, were coinjected, and, again, a synthetic interaction was observed (Figure S3E). These findings together support the proposal that BCL6 maintains LR asymmetry by rendering *Pitx2* expression resistant to the effects of Notch signaling.

In order to determine the molecular mechanism of this BCL6 effect, we sought BCL6-dependent changes in the composition of Notch transcriptional complexes. BCL6 was overexpressed in embryos, and coimmunoprecipitation with α-Notch1 antibody was performed. MAM1, but not Su(H), was replaced by the overexpressed BCL6 protein (Figure 4A). Interaction studies with in vitro-translated proteins demonstrate that this interference by BCL6 was dose dependent (Figure 4B). Conversely, the overexpression of MAM1 and dn-MAM1 displaced BCL6 from the transcriptional complex of Notch signaling (lanes 2 and 4 in Figure 4C). Note that NBD-S and MAM1 (Figure S3B) or dn-MAM1 (Figure 4D) did not exclude each other from the transcriptional complex. It is possible that the NBD-S-binding site in the ANK domain of NICD may not overlap with the MAM1-binding site or/and NBD-S may interact with NICD more strongly than full-length BCL6 because the truncation of other domains may lead to conformation change. These data together demonstrate that BCL6 competes with MAM1 for the ANK domain of NICD to inhibit the transcriptional activity of Notch.

BCL6 Forms a Complex with BCoR

As a previous study in *Xenopus* showed that BCoR is required for the expression of *Pitx2* and LR patterning (Hilton et al., 2007) and *BCoR* was expressed in the LPM at stage 25 (Figure 2C), we examined whether BCoR is present in the Notch/BCL6 complex. When immunoprecipitation with α-Notch1 antibody was performed, BCoR was precipitated with the Notch/BCL6 complex (Figure 4E). When BCL6 was knocked down by BCL6 MO, the amount of BCoR precipitated by α-Notch1 antibody was reduced (Figure 4F), suggesting that BCL6 recruits BCoR into the transcriptional complex of Notch signaling. To examine whether BCoR is functionally involved in the suppression of Notch signaling, the enhancement of BCL6 effect by BCoR in *Pitx2* expression was tested. The number of *Pitx2*-expressing embryos in the coinjection of *GR-NICD* and *mBCL6-GR* was increased by the coinjection of *BCoR* (lanes 3 and 5 in Figure 4G). Indeed, the overexpression of BCoR itself was sufficient to attenuate NICD's effects on *Pitx2* (lane 4 in Figure 4G), and this BCoR activity was dependent on endogenous BCL6 (lane 6 in Figure 4G). Collectively, our data indicate that BCL6 inhibits Notch-dependent transcription by blocking NICD/Su(H) interactions with the coactivator MAM1 and recruiting the corepressor BCoR instead.

ESR1 Is a Notch Target Gene Suppressed by BCL6 during LR Patterning

In an effort to refine our model for BCL6 action, we looked for direct target genes shared by BCL6 and Notch, where we might test the mechanistic model discussed above. The expression of Notch-activated genes in the LPM was therefore examined by RT-PCR. Interestingly, the expression of *ESR1* (Lamar and Kintner, 2005; Wettstein et al., 1997) was barely detected, whereas *Hairy2* (Davis et al., 2001) was expressed (Figure S4A). To test whether BCL6 differentially regulates the transcription of selected Notch target genes, the expression of *ESR1* and *Hairy2* in the BCL6-depleted left LPM was tested by quantitative RT-PCR. The expression of *ESR1*, but not *Hairy2*, was increased in the BCL6-depleted LPM (Figure 5A) and in the nervous system at stage 14 (Figure 5B). This increase of *ESR1* expression by BCL6 MO was decreased by the coinjection of Notch1 MO, suggesting that BCL6 directly regulates the transcriptional output of Notch signaling on *ESR1* (Figure 5C). In addition, an increase of *ESR1* expression by NICD in the left LPM was reduced by the coinjection of BCL6 (Figure S4B).

Next, the possibility that ESR1 mediates Notch signaling to suppress the expression of *Pitx2* was examined. A hormone-inducible *ESR1* (ESR1-GR) or *Hairy2* (Hairy2-GR) RNA was injected into a left dorsal blastomere of 4-cell-stage embryos, and the expression of *Pitx2* was tested. ESR1 (74%, n = 34), but not Hairy2 (4%, n = 28), suppressed *Pitx2* expression (Figure 5D; Figure S4C). To examine whether ESR1 is the primary mediator of Notch effects on *Pitx2*, ESR1 was knocked down with an MO (ESR1 MO) (Figure S4D). However, the ESR1 MO was not able to rescue *Pitx2* expression in BCL6 MO coinjected embryos, indicating that other Notch target genes that converge on *Pitx2* are also suppressed by BCL6 in the left LPM (Figure 5E; Figure S4E).

Chromatin immunoprecipitation (ChIP) assays with nuclear extracts isolated from stage-25 embryos confirmed that Notch1 is associated with the known CSL-binding sites at the *ESR1* and *Hairy2* genomic loci; however, BCL6 bound only the *ESR1* CSL-binding element (Figure 6A). We next examined whether BCL6 recruitment is dependent on the NICD. dn-Su(H) was used for this study, because overexpressed dn-Su(H) dominantly interacts with NICD but cannot bind the CSL-binding site (Wettstein et al., 1997). dn-Su(H) overexpression prevented both Notch1 (lanes 7 and 8 in Figure 6B) and BCL6 (lanes 5 and 6 in Figure 6B) from binding the *ESR1* CSL-binding site. However, BCL6 MO increases MAM1 occupancy of *ESR1* CSL-binding site (lanes 5 and 6 in Figure 6C) without affecting NICD (lanes 7 and 8 in Figure 6C). These data strongly suggest that BCL6 binds to the transcriptional complex present at the CSL-binding site of *ESR1* through NICD and competes with MAM1. However, it still remains possible that BCL6 interacts directly with the *ESR1* gene, at elements other than the CSL-binding site tested above.

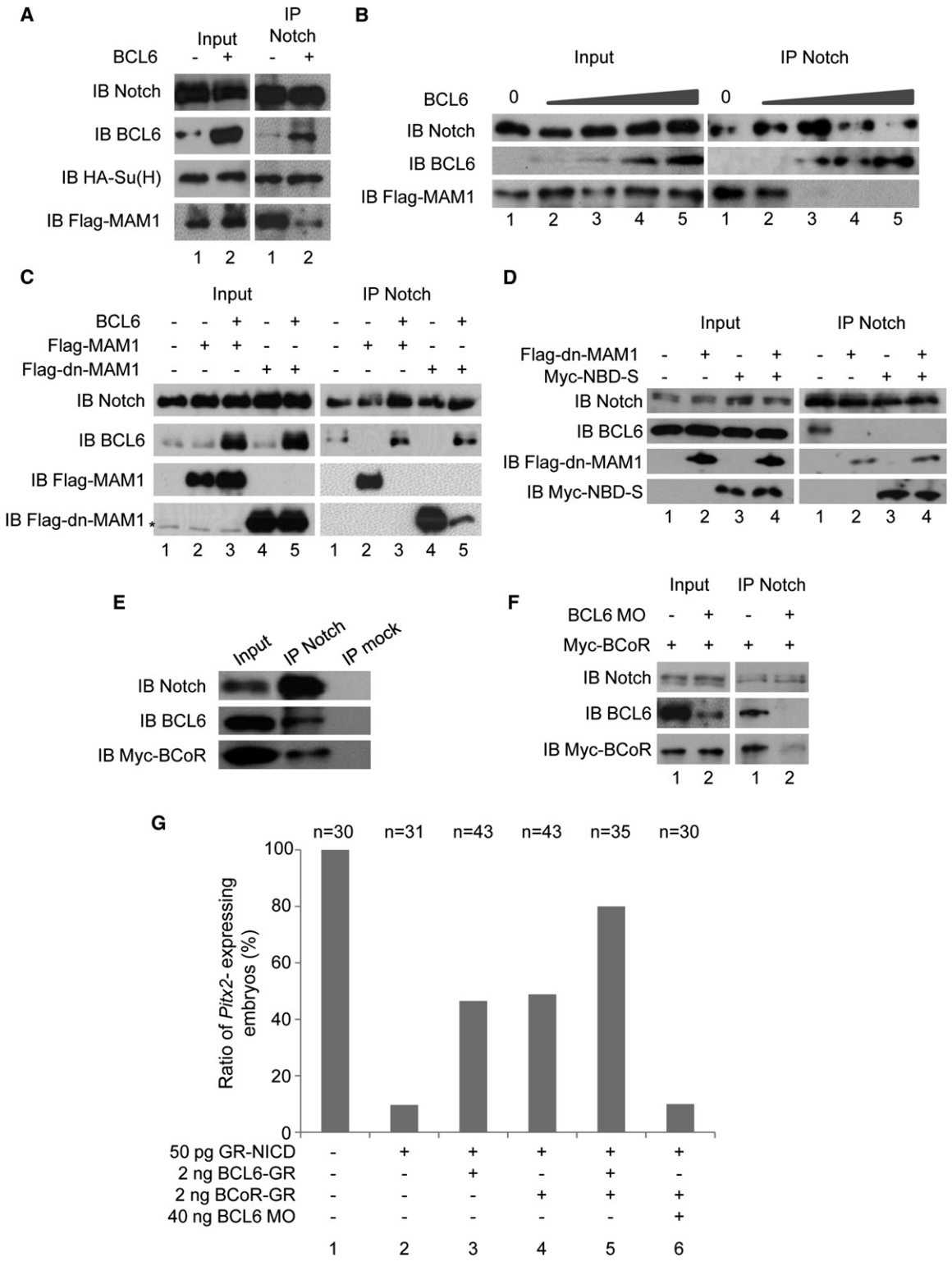

Figure 4. The Mechanisms by Which the BCL6/BCoR Complex Blocks Notch-Dependent Transcription

(A) HA-tagged Su(H), Flag-tagged MAM1, or/and BCL6 was expressed in embryos, and protein extracts were isolated from 50 embryos at stage 10. Coimmunoprecipitation with α-Notch antibody was performed.

(B) Coimmunoprecipitation with in vitro-synthesized proteins.

(C and D) Flag-tagged MAM1, Flag-tagged dn-MAM1, BCL6, or/and Myc-tagged NBD-S was expressed in embryos, and protein extracts were isolated from 50 embryos at stage 10 for each experiment.

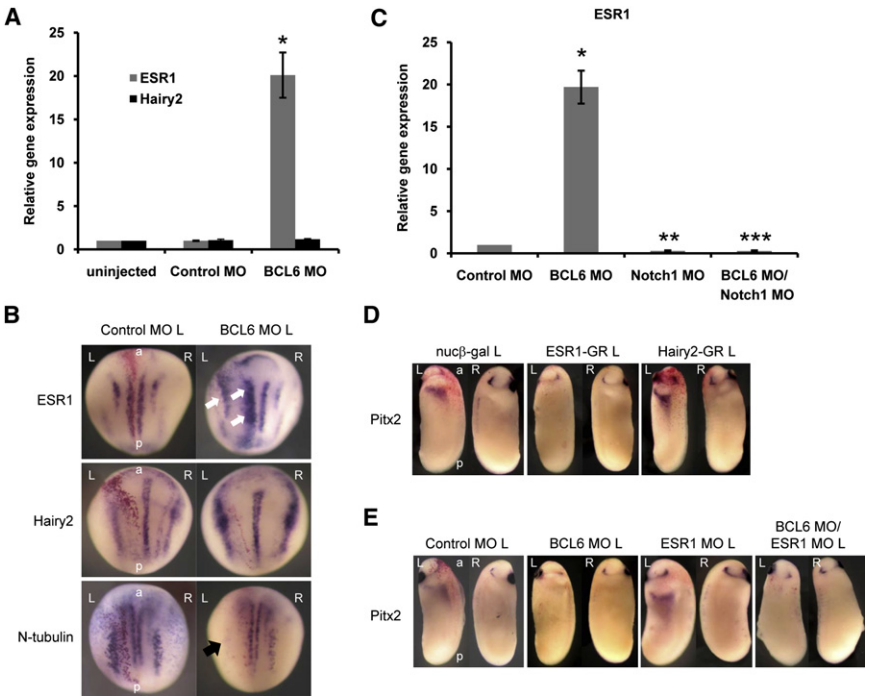

Figure 5. *ESR1* Is a Target of BCL6 during LR Patterning and Neural Development

(A) BCL6 MO was injected into the left side of embryos, and left LPM tissues were dissected from 20 embryos at stage 25 for quantitative RT-PCR. The injection side was traced by the coinjection of *GFP* (data not shown). *p < 0.05, n = 3.

(B) BCL6 MO was injected into a dorsal blastomere of four-cell-stage embryos, and embryos were fixed at stage 14. Increased *ESR1* expression and decreased *N-tubulin* expressions are indicated by white and black arrows, respectively.

(C) BCL6 MO or/and Notch1 MO was injected into the left side of embryos, and left LPM tissues were dissected from 20 embryos at stage 25 for quantitative RT-PCR. *p < 0.01, n = 3; **p < 0.01, n = 3; ***p < 0.01, n = 3.

(D) 1 ng *ESR1-GR* or *Hairy2-GR* was injected for each experiment.

(E) 40 ng ESR1 MO or/and BCL6 MO was injected for each experiment. The injected side is indicated by "L" (left) beside the names of the injected samples. L, left; R, right; a, anterior; p, posterior.

All error bars shown are standard deviation (SD) from the mean of triplicates.

To search for a BCL6-response element, 2367 bp of the *Xenopus tropicalis ESR1* genomic locus was amplified by PCR with primers designed with *X. tropicalis* genome sequences (University of California Santa Cruz Genome Bioinformatics; http://genome.ucsc.edu/) and linked to the luciferase reporter (pGL3-ESR1P-2367). After this construct was coinjected with *NICD* or/and *BCL6/BCoR* RNA into *Xenopus* embryos, the luciferase activity was measured. Increased luciferase activity by NICD was decreased by the coinjection of BCL6 and BCoR, suggesting that this fragment of the *ESR1* gene includes the BCL6-response element (Figure 6D; Figure S5A). A deletion analysis of this genomic fragment revealed that the BCL6-response element was present between −1072 and −740 (Figure 6D; Figure S5A); however, consensus BCL6-binding sequences as published previously (Chang et al., 1996) were not found between −1072 and −740. Electrophoretic mobility shift assays (EMSA) were therefore performed with full-length or the C2H2-type zinc finger domain of BCL6 recombinant protein (GST-BCL6 or GST-ZF) to identify the BCL6-response element in this region of *ESR1*. Several probes for EMSA were designed in the candidate region of *ESR1* (−1072/−740) and were radiolabeled by PCR. The −1030/−897 probe resulted in a BCL6-retarded band (lane 3: GST-BCL6; lane 4: GST-ZF in Figure 6E). Because BCL6 directly interacts with this probe, we will refer to the corresponding region of *ESR1* as the BCL6-response element (see Figure 6D). Indeed, the overexpression of the zinc finger domain of BCL6 (BCL6-ZF) could inhibit the expression of *Pitx2*, indicating that BCL6-ZF competes with endogenous BCL6 for the BCL6-binding site and inhibits the function of BCL6 by displacing endogenous BCL6 from the *ESR1* locus (Figure 6F). Because two nonoverlapping fragments (5′ response element and 3′ response element) of the BCL6-response element (Figure S5B) could each interact with GST-ZF, there is likely more than one BCL6-binding site in the BCL6-response element (Figure S5C). These results indicate that direct binding of BCL6 to both the target locus and the NICD is required for its ability to shut down Notch target gene expression. These findings, in turn, suggest a mechanism by which selective inhibition of specific Notch-activated target genes is achieved.

DISCUSSION

We have uncovered that BCL6 recruits BCoR and blocks the transcription of selected Notch target genes to maintain *Pitx2* expression and LR asymmetry in *Xenopus* (Figure 7A). It should be noted that mutations of human BCoR result in the Oculofaciocardiodental (OFCD) syndrome, which is characterized by defective lateralization, including dextrocardia, asplenia, and intestinal malrotation (Hilton et al., 2007; Ng et al., 2004). These findings indicate that the dysfunction of BCL6 in mammals can likely lead to defects of LR asymmetry. However, the defects of LR asymmetry in BCL6-deficient mice have not been reported. BCL6-deficient mice displayed defective GC development and a selective defect in T cell-dependent antibody responses (Ye et al., 1997), and also developed myocarditis and pulmonary vasculitis (Dent et al., 1997; Ye et al., 1997; Yoshida et al., 1999).

(E and F) Myc-tagged BCoR was expressed in embryos (E) without or (F) with the BCL6 MO, and protein extracts were isolated from 50 embryos at stage 10. Coimmunoprecipitation with α-Notch antibody was performed. α-vimentin antibody was used for a mock immunoprecipitation.

(G) The expression of *Pitx2* at stage 25 was tested by whole-mount in situ hybridization, and the ratios of the *Pitx2*-expressing embryo number versus the total tested embryo number are shown. Total numbers of each injection are shown as "n" on the top of each bar.

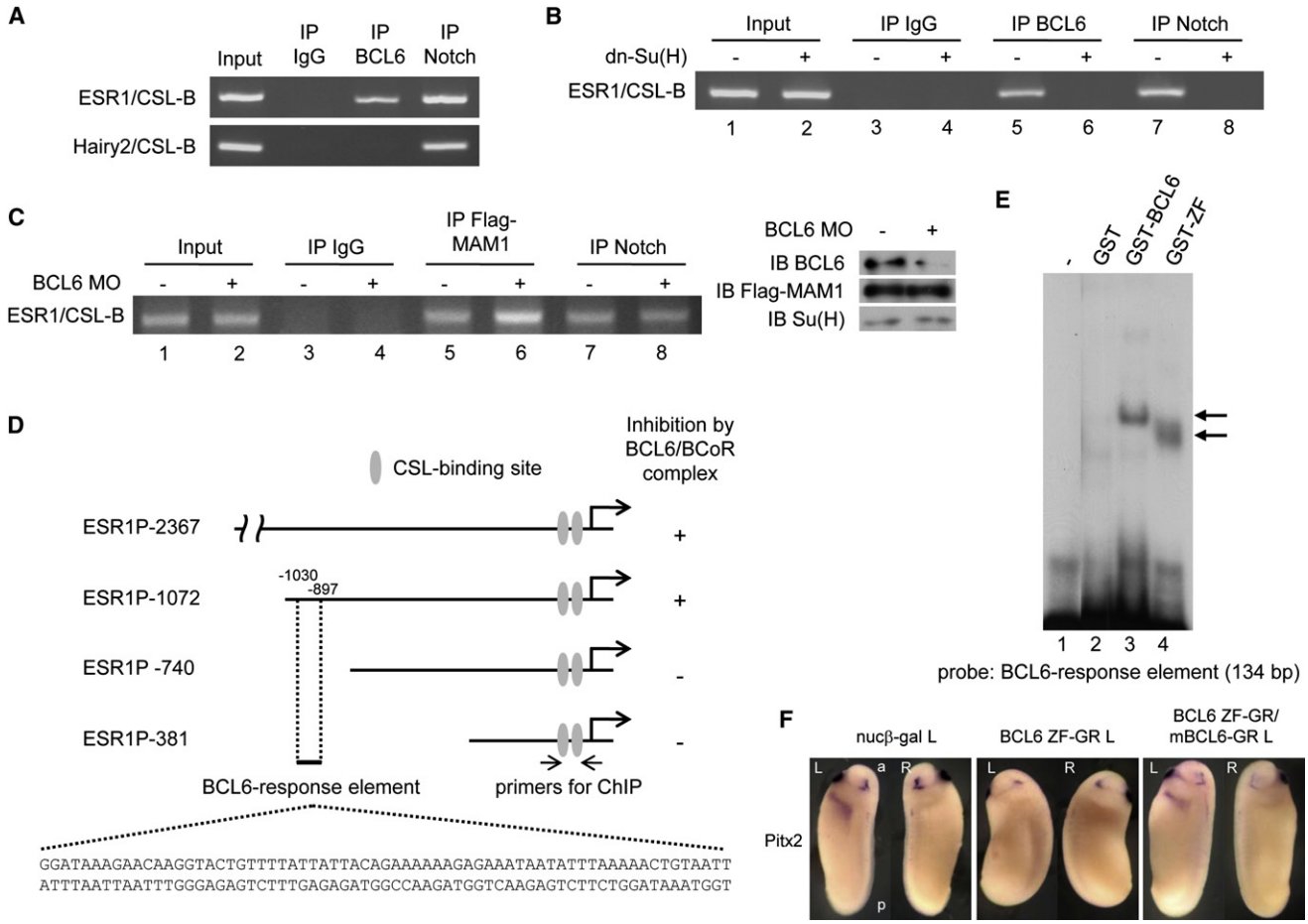

Figure 6. The Mechanisms by Which BCL6 Shuts Down the Expression of Selected Notch Target Genes

(A) ChIP assays were performed with nuclear extracts from stage-25 embryos by using α-BCL6 antibody, α-Notch1 antibody, or mouse IgG. Mouse IgG was used for a mock ChIP assay.

(B) 2 ng *dn-Su(H)* was injected into two-cell-stage embryos, and nuclear extracts were isolated at stage 10 for ChIP assays.

(C) BCL6 MO or/and 1 ng *Flag-MAM1* was injected into two-cell-stage embryos, and nuclear extracts were isolated at stage 10 for ChIP assays. The levels of input proteins were confirmed by immunoblotting.

(D) Deleted fragments of the *X. tropicalis ESR1* gene were linked to the luciferase reporter. Numbers indicate the position of nucleotides from the initiation site.

(E) Incubation of GST-BCL6 or GST-ZF with a probe corresponding to a 134 bp (−1030/−897) element yielded one distinct retarded band indicated by an arrow.

(F) 2 ng *BCL6 ZF-GR* or/and *mBCL6-GR* was injected for each experiment. The injected side is indicated by "L" (left) beside the names of the injected samples. L, left; R, right; a, anterior; p, posterior.

Based on our findings and the observation in human syndrome, it remains possible that defects of LR asymmetry in BCL6-deficient mice may have been overlooked because defects of LR asymmetry are not lethal (Peeters and Devriendt, 2006). The reexamination of BCL6-deficient mice will be required to address this important question.

In mice, distinct asymmetric expression of *Delta-like 1* (*Dll1*), *Notch1*, and *Notch2* around the node (Bettenhausen et al., 1995; Krebs et al., 2003; Raya et al., 2003; Williams et al., 1995) and asymmetric Notch activation have not been reported. In *Dll1* knockout or *Notch1* and *Notch2* double-knockout mice, the symmetric expression of *Nodal* in the perinodal region is completely abolished, and these mice show defects of LR asymmetry (Krebs et al., 2003; Raya et al., 2003). Similar to the studies in mice, any LR asymmetry in the expression of *Delta1*, *Serrate1*, and *Notch1* around the *Xenopus* GRP was not observed (Figure S2G), and the symmetric expression of *Xnr1* on the GRP was inhibited by the depletion of *Xenopus* Notch1 (Figure 2D; Figure S2I). These findings indicate that *Xenopus* Notch1 initiates symmetric *Xnr1* expression around the GRP required for LR patterning, and these mechanisms are conserved between mice and *Xenopus*. However, it still remains unclear whether asymmetric Notch activity exists around the GRP. It is possible that other signals, including the generation of a leftward fluid flow in or close to the GRP by the rotation of cilia (Schweickert et al., 2007), together could break the bilateral symmetry and induce the left-specific *Xnr1* expression in the LPM. In contrast, studies in chick have shown that the expression of *Dll1* around the left side of Hensen's node is stronger than the right, and that asymmetric activity of Notch signaling on the left side of the node regulates the left-side expression of *Nodal* (Raya et al., 2004). It remains very likely that the precise role of Notch

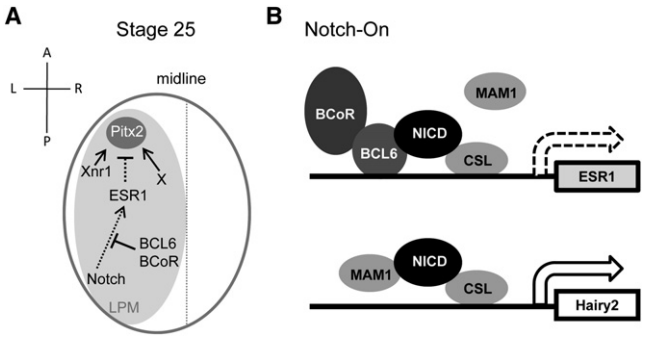

Figure 7. A Model for the Regulation of Notch Signaling by the BCL6/BCoR Complex during LR Patterning

(A) At stage 25, the BCL6/BCoR complex inhibits Notch's ability to suppress *Pitx2* expression initiated by Xnr1-dependent and -independent signals and maintains LR asymmetry.

(B) Sequence-specific targeting of BCL6 to a subset of Notch-activated genes occurs by an unknown mechanism. Once recruited, however, BCL6 both competes MAM1 away from the locus and recruits BCoR, effectively blocking Notch-dependent transcription.

signaling in the patterning of LR asymmetry may be slightly different among species.

We have shown that the expression of *Pitx2* on the left LPM is dually regulated in Nodal (Xnr1)-dependent and -independent manners. The expression of *Pitx2* in the absence of Nodal function has been reported in *Notch1* and *Notch2* knockout mice (Krebs et al., 2003; Raya et al., 2003), mutations of mouse PDK2 (Pennekamp et al., 2002), and FURIN-deficient mice (Constam and Robertson, 2000). These findings suggest that *Pitx2* expression is regulated in part by Nodal-independent mechanisms. As we have found that *Pitx2* expression is significantly suppressed by loss of BCL6 or by the overexpression of *NICD* or *ESR1* in *Xenopus* embryos, this indicates that a Notch-ESR1 signal could simultaneously inhibit Nodal-dependent and -independent signals to suppress the expression of *Pitx2* (Figure S3A). However, how the Notch-ESR1 signal inhibits these signals still remains unknown. Interestingly, the Nodal-dependent expression of mouse *Pitx2* is controlled by a two-step mechanism during the patterning of LR asymmetry (Shiratori et al., 2001). Nodal signal acting in cooperation with the transcription factor FAST-1 is required to initiate left-side-specific expression of mouse *Pitx2*; however, the relevant left-side-specific enhancer is also dependent on Nkx2.5 to maintain activation. All of these enhancer sequences are conserved at the *Xenopus Pitx2* locus (Shiratori et al., 2001), suggesting that the left-specific expression of *Xenopus Pitx2* is regulated by the same two-step mechanism. ESR1 may directly bind this left-side-specific enhancer of *Pitx2* and shut down *Pitx2* expression, although an indirect inhibition cannot be excluded. It will therefore be important to investigate in future studies which regulatory step of *Pitx2* induction is inhibited by the Notch-ESR1 cascade and how ESR1 inhibits *Pitx2* expression.

How does Notch signaling activate only the correct target genes in the LPM? One may posit that distinct repressors expressed in the LPM may play a crucial role in inhibiting the transcription of unnecessary target genes during LPM development, and that BCL6 must be such a factor. Indeed, our studies show that the expression of *ESR1*, but not *Hairy2*, was selectively inhibited by BCL6, and that ESR1, but not Hairy2, inhibited the expression of *Pitx2* (Figure 5). BCL6 directly interacts with the *ESR1 cis*-regulatory element (Figure 6) and competes with MAM1 for the ANK domain of Notch1 to shut down the transcription of *ESR1* when Notch signaling is activated (Figure 7B). Although 134 bp of the BCL6-response element at the *ESR1* locus was identified, consensus BCL6-binding sequences (Chang et al., 1996) were not found in this element (Figure 6D). It is possible that BCL6 may interact with the *ESR1* element through slightly different binding sequences. Our study suggests that there are multiple BCL6-binding sites in the BCL6-response element of *ESR1* (Figure S5C). Therefore, a further analysis of this element remains necessary to identify the BCL6-binding site(s) and address how BCL6 is recruited to the *ESR1* locus.

Our data define an important mechanism by which BCL6 constrains Notch signaling to provide cell-type-appropriate outputs. Because the expression of *Notch1* overlaps with that of *BCL6* in diverse ectodermal and mesodermal tissues, including the eye, the nervous system, and the somites (Figure S2A)—and, indeed, both Notch signaling and BCL6 abnormalities have been implicated in leukemias—this regulatory mechanism may be important for other developmental, homeostatic, or pathophysiological processes.

EXPERIMENTAL PROCEDURES

Embryo Manipulations

Eggs were artificially fertilized by using testis homogenate and cultivated in 0.1× Marc's Modified Ringer's solution (MMR) (Peng, 1991). Embryos were staged according to Nieuwkoop and Faber (1967).

GST Pull-Down and Protein Identification by Mass Spectrometry

GST fusion proteins were produced in *E. coli* strain BL21. The bacterial cells were disrupted by sonication in Phosphate Buffered Saline (PBS) with protease inhibitor cocktail (EDTA-free Complete Mini, Roche Applied Science). To purify the GST fusion proteins, glutathione-conjugated agarose beads (Sigma) were added to those samples and incubated at 4°C for 1 hr. The beads were washed three times with 1% Triton-X in PBS buffer. For our screen, GST fusion protein was additionally washed with lysate buffer (20 mM Tris-HCl [pH 8.0], 5 mM $MgCl_2$, 1 mM EDTA, 50 mM KCl, 0.1% Triton X-100, 10% glycerol, and 1 mM dithiothreitol). Stage-15 to -25 embryos were homogenized in lysate buffer containing protease inhibitors to isolate embryonic protein extracts. The beads with GST or GST-ANK protein were incubated with embryonic protein extracts at 4°C for 4 hr. The samples were washed five times with lysate buffer without glycerol. After the washes, the proteins associated with GST or GST-ANK were eluted with elution buffer (200 mM Tris-HCl [pH 8.0], 4 mM $MgCl_2$, 0.8 mM EDTA, 40 mM KCl, 0.08% Triton X-100, 0.8 mM dithiothreitol, 10 mM glutathione, and protease inhibitors) at 4°C for 1 hr. The eluted samples were separated by sodium dodecyl sulfate polyacrylamide gel electrophoresis (SDS-PAGE). The gel was stained with the Silver Stain Plus kit (Bio-Rad). The candidate protein bands were excised from the gel, digested with trypsin, and analyzed with matrix-assisted laser desorption/ionization time-of-flight mass spectrometry (MALDI-TOF-MS). The identification of candidate proteins was determined by the MASCOT search algorithm (http://www.matrixscience.com). The monoisotopic peptide masses were used to search the SwissProt database within a mass tolerance of ±0.2 Da for *Xenopus laevis* protein, and one missed cleavage was allowed.

Immunoprecipitation and Immunoblotting

Embryos were homogenized in lysate buffer, and embryonic protein extracts were used for immunoprecipitation. The embryonic protein extracts were incubated with an antibody at 4°C overnight. α-Notch (Developmental Studies Hybridoma Bank [DSHB]), α-BCL6 (R&D Systems, Inc.), α-RBP-Jκ

(for Su(H): Santa Cruz Biotechnology, Inc.), α-Flag (Sigma), α-HA (Santa Cruz Biotechnology, Inc.), α-Myc (Santa Cruz Biotechnology, Inc.), and α-vimentin (DSHB) antibodies were used for immunoprecipitation or immunoblotting. All in vitro-translated proteins were synthesized by the TNT Coupled Reticulocyte Lysate System (Promega) for immunoprecipitation studies.

Microinjection of Synthetic RNA and Morpholino Antisense Oligo

Capped synthetic mRNAs were generated by in vitro transcription with SP6 polymerase, using the mMessage mMachine kit (Ambion, Inc.). Morpholino Antisense Oligos (MO) were designed and produced by Gene Tools, LLC. For microinjections, embryos were transferred to 3% Ficoll 400 in 0.1× MMR, and injected embryos were cultured in 0.1× MMR until the desired stage. In all injection studies, 100 pg *GFP* RNA for observing phenotypes or 250 pg *nucβ-gal* RNA (red color) for whole-mount in situ hybridization was injected for a tracer of injection. For the activation of GR-fused protein, dexamethasone (DEX: final concentration 10 μM) was added to the medium. Details of plasmid construction and sequences of MOs are presented in the Supplemental Experimental Procedures.

β-Galactosidase Staining and Whole-Mount In Situ Hybridization

Embryos were fixed with gal fix solution (2% formaldehyde, 0.2% glutaraldehyde, 0.02% Triton-X, 0.01% sodium deoxycholate in PBS) on ice for 30 min. Galactosidase activity was visualized with the RedGal substrate (Research Organics) in staining buffer (5 mM $K_3[Fe(CN)_6]$, 5 mM $K_4[Fe(CN)_6]$, 2 mM $MgCl_2$ in PBS). After staining, embryos were refixed with MEMFA (0.1 M MOPS, 2 mM EGTA [pH 8.0], 1 mM $MgSO_4$, and 3.7% formaldehyde) for 30 min. Whole-mount in situ hybridization was performed essentially as described previously (Harland, 1991; Takada et al., 2005) by using Digoxigenin (Roche Applied Science)-labeled antisense RNA probes and BM purple (Roche Applied Science) for the chromogenic reaction. Information on probes is presented in the Supplemental Experimental Procedures.

RT-PCR Analysis

Total RNA was isolated by the method with 200 μg/ml Proteinase K described previously (Hilz et al., 1975). Reverse transcriptase (RT) reaction for the synthesis of cDNA was performed with Superscript II (Invitrogen) according to the manufacturer's instructions. Specimens were analyzed for gene expression levels using regular PCR with Taq DNA polymerase (New England Biolabs) or the iQ5 Real-Time PCR Detection System (Bio-Rad) with the QuantiTect SYBR Green PCR kit (QIAGEN). Information on primers is presented in the Supplemental Experimental Procedures. All error bars shown are the standard deviation (SD) from the mean of triplicates.

Chromatin Immunoprecipitation

Chromatin immunoprecipitation (ChIP) assays were performed with a kit from Millipore (Kato et al., 2002; Sachs and Shi, 2000). Nuclei were isolated as described previously (Almouzni et al., 1994). The isolated nuclei were resuspended in 360 μl nucleus isolation buffer (0.25 M sucrose, 10 mM Tris-HCl [pH 7.5], 3 mM $CaCl_2$, and protease inhibitor cocktail). Proteins were cross-linked to DNA by adding formaldehyde (final concentration: 1%) and incubated on ice for 10 min and at room temperature for 20 min. After centrifuging samples, the nuclei were resuspended in 200 μl lysis buffer (1% SDS, 50 mM Tris-HCl [pH 8.1], 10 mM EDTA, protease inhibitor cocktail) on ice for 10 min. The lysate was sonicated ten times with 10 s pulses by using a sonicator (Branson Sonifier 450, VWR) set to 50% of maximum power to reduce DNA length to between 200 and ~1,000 bp. After debris was removed, DNA was quantified and adjusted to equal concentration for PCR. Information of primers is presented in the Supplemental Experimental Procedures. One milliliter of chromatin solution was used for each ChIP assay with α-BCL6, α-Notch1, or α-Flag antibody. One percentage of chromatin solution was stored for the input DNA.

Luciferase Reporter Assay

Luciferase reporter constructs of the *ESR1* gene were generated by subcloning different lengths of genomic fragments, between −1 and −2367, into pGL3 basic vector (Promega), and pRL-CMV (Promega) was used for the internal control. Luciferase activity was measured by using the Dual Luciferase Reporter Assay System (Promega). All error bars shown are the SD from the mean of triplicates. *X. tropicalis* genomic DNA was gifted by Dr. K. Tamai.

Electrophoretic Mobility Shift Assay

The electrophoretic mobility shift assay was performed as described (Huang et al., 1995). Recombinant proteins, which were eluted from glutathione-conjugated agarose beads by prereaction buffer (50 mM Tris-HCl [pH 8.0], 50 mM KCl, 1 mM EDTA, 1 mM EGTA, 5 mM dithiothreitol, 20% glycerol, 10 mM glutathione, and protease inhibitors), were incubated for 10 min on ice in a 15 μl reaction volume containing 50 mM Tris-HCl (pH 8.0), 50 mM KCl, 7.5 mM Mg_2Cl, 1 mM EDTA, 1 mM EGTA, 5 mM dithiothreitol, 20% glycerol, 50 μg/ml poly (dI-dC), and protease inhibitors. A ^{32}P-labeled probe was added, and incubation continued for 15 min on ice. The protein-DNA complex was separated by electrophoresis through a 6% native polyacrylamide gel.

SUPPLEMENTAL INFORMATION

Supplemental Information includes five figures and Supplemental Experimental Procedures and are available with this article online at doi:10.1016/j.devcel.2009.12.023.

ACKNOWLEDGMENTS

We thank C. Kintner, M. Mercola, C.V.E. Wright, D.L. Turner, M. Levin, N. Ueno, T. Kinoshita, H. Sive, K. Tamai, R. Habas, and the National Institute for Basic Biology (NIBB) for plasmids, and the Developmental Studies Hybridoma Bank (DSHB) for antibodies. We also thank J. Horabin and R. Habas for critical suggestions on the manuscript. This work was supported by the Bankhead-Coley Cancer Research Program, Florida State University Council on Research and Creativity (CRC) planning grant, and the National Institute of Child Health and Human Development (NICHD) (HD052526).

Received: December 19, 2008
Revised: October 15, 2009
Accepted: December 22, 2009
Published: March 15, 2010

REFERENCES

Adachi, H., Saijoh, Y., Mochida, K., Ohishi, S., Hashiguchi, H., Hirao, A., and Hamada, H. (1999). Determination of left/right asymmetric expression of nodal by a left side-specific enhancer with sequence similarity to a lefty-2 enhancer. Genes Dev. *13*, 1589–1600.

Albagli-Curiel, O. (2003). Ambivalent role of BCL6 in cell survival and transformation. Oncogene *22*, 507–516.

Almouzni, G., Khochbin, S., Dimitrov, S., and Wolffe, A.P. (1994). Histone acetylation influences both gene expression and development of *Xenopus laevis*. Dev. Biol. *165*, 654–669.

Baron, B.W., Nucifora, G., McCabe, N., Espinosa, R., 3rd, Le Beau, M.M., and McKeithan, T.W. (1993). Identification of the gene associated with the recurring chromosomal translocations t(3;14)(q27;q32) and t(3;22)(q27;q11) in B-cell lymphomas. Proc. Natl. Acad. Sci. USA *90*, 5262–5266.

Bettenhausen, B., Hrabe de Angelis, M., Simon, D., Guenet, J.L., and Gossler, A. (1995). Transient and restricted expression during mouse embryogenesis of Dll1, a murine gene closely related to *Drosophila* Delta. Development *121*, 2407–2418.

Boorman, C.J., and Shimeld, S.M. (2002). The evolution of left-right asymmetry in chordates. Bioessays *24*, 1004–1011.

Borggrefe, T., and Oswald, F. (2009). The Notch signaling pathway: transcriptional regulation at Notch target genes. Cell. Mol. Life Sci. *66*, 1631–1646.

Branford, W.W., Essner, J.J., and Yost, H.J. (2000). Regulation of gut and heart left-right asymmetry by context-dependent interactions between *Xenopus* lefty and BMP4 signaling. Dev. Biol. *223*, 291–306.

Brennan, J., Norris, D.P., and Robertson, E.J. (2002). Nodal activity in the node governs left-right asymmetry. Genes Dev. *16*, 2339–2344.

Capdevila, J., Vogan, K.J., Tabin, C.J., and Izpisua Belmonte, J.C. (2000). Mechanisms of left-right determination in vertebrates. Cell *101*, 9–21.

Chang, C.C., Ye, B.H., Chaganti, R.S., and Dalla-Favera, R. (1996). BCL-6, a POZ/zinc-finger protein, is a sequence-specific transcriptional repressor. Proc. Natl. Acad. Sci. USA *93*, 6947–6952.

Constam, D.B., and Robertson, E.J. (2000). Tissue-specific requirements for the proprotein convertase furin/SPC1 during embryonic turning and heart looping. Development *127*, 245–254.

Davis, R.L., Turner, D.L., Evans, L.M., and Kirschner, M.W. (2001). Molecular targets of vertebrate segmentation: two mechanisms control segmental expression of *Xenopus* hairy2 during somite formation. Dev. Cell *1*, 553–565.

Dent, A.L., Shaffer, A.L., Yu, X., Allman, D., and Staudt, L.M. (1997). Control of inflammation, cytokine expression, and germinal center formation by BCL-6. Science *276*, 589–592.

Diederich, R.J., Matsuno, K., Hing, H., and Artavanis-Tsakonas, S. (1994). Cytosolic interaction between deltex and Notch ankyrin repeats implicates deltex in the Notch signaling pathway. Development *120*, 473–481.

Hamada, H., Meno, C., Watanabe, D., and Saijoh, Y. (2002). Establishment of vertebrate left-right asymmetry. Nat. Rev. Genet. *3*, 103–113.

Harland, R.M. (1991). In situ hybridization: an improved whole-mount method for *Xenopus* embryos. Methods Cell Biol. *36*, 685–695.

Heasman, J., Kofron, M., and Wylie, C. (2000). β-catenin signaling activity dissected in the early *Xenopus* embryo: a novel antisense approach. Dev. Biol. *222*, 124–134.

Hilton, E.N., Manson, F.D., Urquhart, J.E., Johnston, J.J., Slavotinek, A.M., Hedera, P., Stattin, E.L., Nordgren, A., Biesecker, L.G., and Black, G.C. (2007). Left-sided embryonic expression of the BCL-6 corepressor, BCOR, is required for vertebrate laterality determination. Hum. Mol. Genet. *16*, 1773–1782.

Hilz, H., Wiegers, U., and Adamietz, P. (1975). Stimulation of proteinase K action by denaturing agents: application to the isolation of nucleic acids and the degradation of 'masked' proteins. Eur. J. Biochem. *56*, 103–108.

Huang, H.C., Murtaugh, L.C., Vize, P.D., and Whitman, M. (1995). Identification of a potential regulator of early transcriptional responses to mesoderm inducers in the frog embryo. EMBO J. *14*, 5965–5973.

Huynh, K.D., Fischle, W., Verdin, E., and Bardwell, V.J. (2000). BCoR, a novel corepressor involved in BCL-6 repression. Genes Dev. *14*, 1810–1823.

Jones, C.M., Kuehn, M.R., Hogan, B.L., Smith, J.C., and Wright, C.V. (1995). Nodal-related signals induce axial mesoderm and dorsalize mesoderm during gastrulation. Development *121*, 3651–3662.

Kato, H., Taniguchi, Y., Kurooka, H., Minoguchi, S., Sakai, T., Nomura-Okazaki, S., Tamura, K., and Honjo, T. (1997). Involvement of RBP-J in biological functions of mouse Notch1 and its derivatives. Development *124*, 4133–4141.

Kato, Y., Habas, R., Katsuyama, Y., Naar, A.M., and He, X. (2002). A component of the ARC/Mediator complex required for TGF β/Nodal signalling. Nature *418*, 641–646.

Kawakami, Y., Raya, A., Raya, R.M., Rodriguez-Esteban, C., and Belmonte, J.C. (2005). Retinoic acid signalling links left-right asymmetric patterning and bilaterally symmetric somitogenesis in the zebrafish embryo. Nature *435*, 165–171.

Kerckaert, J.P., Deweindt, C., Tilly, H., Quief, S., Lecocq, G., and Bastard, C. (1993). LAZ3, a novel zinc-finger encoding gene, is disrupted by recurring chromosome 3q27 translocations in human lymphomas. Nat. Genet. *5*, 66–70.

Kiyota, T., and Kinoshita, T. (2002). Cysteine-rich region of X-Serrate-1 is required for activation of Notch signaling in *Xenopus* primary neurogenesis. Int. J. Dev. Biol. *46*, 1057–1060.

Krebs, L.T., Iwai, N., Nonaka, S., Welsh, I.C., Lan, Y., Jiang, R., Saijoh, Y., O'Brien, T.P., Hamada, H., and Gridley, T. (2003). Notch signaling regulates left-right asymmetry determination by inducing Nodal expression. Genes Dev. *17*, 1207–1212.

Kurooka, H., Kuroda, K., and Honjo, T. (1998). Roles of the ankyrin repeats and C-terminal region of the mouse notch1 intracellular region. Nucleic Acids Res. *26*, 5448–5455.

Lamar, E., and Kintner, C. (2005). The Notch targets Esr1 and Esr10 are differentially regulated in *Xenopus* neural precursors. Development *132*, 3619–3630.

Levin, M. (2005). Left-right asymmetry in embryonic development: a comprehensive review. Mech. Dev. *122*, 3–25.

Li, Z., Wang, X., Yu, R.Y., Ding, B.B., Yu, J.J., Dai, X.M., Naganuma, A., Stanley, E.R., and Ye, B.H. (2005). BCL-6 negatively regulates expression of the NF-κB1 p105/p50 subunit. J. Immunol. *174*, 205–214.

Lohr, J.L., Danos, M.C., and Yost, H.J. (1997). Left-right asymmetry of a nodal-related gene is regulated by dorsoanterior midline structures during *Xenopus* development. Development *124*, 1465–1472.

Lustig, K.D., Kroll, K., Sun, E., Ramos, R., Elmendorf, H., and Kirschner, M.W. (1996). A *Xenopus* nodal-related gene that acts in synergy with noggin to induce complete secondary axis and notochord formation. Development *122*, 3275–3282.

Matsuno, K., Diederich, R.J., Go, M.J., Blaumueller, C.M., and Artavanis-Tsakonas, S. (1995). Deltex acts as a positive regulator of Notch signaling through interactions with the Notch ankyrin repeats. Development *121*, 2633–2644.

Matsuno, K., Eastman, D., Mitsiades, T., Quinn, A.M., Carcanciu, M.L., Ordentlich, P., Kadesch, T., and Artavanis-Tsakonas, S. (1998). Human deltex is a conserved regulator of Notch signalling. Nat. Genet. *19*, 74–78.

Ng, D., Thakker, N., Corcoran, C.M., Donnai, D., Perveen, R., Schneider, A., Hadley, D.W., Tifft, C., Zhang, L., Wilkie, A.O., et al. (2004). Oculofaciocardiodental and Lenz microphthalmia syndromes result from distinct classes of mutations in BCOR. Nat. Genet. *36*, 411–416.

Nieuwkoop, P.D., and Faber, J. (1967). Normal Table of *Xenopus laevis* (Daudin) (Amsterdam, The Netherlands: North-Holland Publishing Co).

Niu, H., Cattoretti, G., and Dalla-Favera, R. (2003). BCL6 controls the expression of the B7-1/CD80 costimulatory receptor in germinal center B cells. J. Exp. Med. *198*, 211–221.

Norris, D.P., and Robertson, E.J. (1999). Asymmetric and node-specific nodal expression patterns are controlled by two distinct *cis*-acting regulatory elements. Genes Dev. *13*, 1575–1588.

Ohi, Y., and Wright, C.V. (2007). Anteriorward shifting of asymmetric Xnr1 expression and contralateral communication in left-right specification in *Xenopus*. Dev. Biol. *301*, 447–463.

Ohno, H. (2004). Pathogenetic role of BCL6 translocation in B-cell non-Hodgkin's lymphoma. Histol. Histopathol. *19*, 637–650.

Palmer, A.R. (2004). Symmetry breaking and the evolution of development. Science *306*, 828–833.

Pasqualucci, L., Bereschenko, O., Niu, H., Klein, U., Basso, K., Guglielmino, R., Cattoretti, G., and Dalla-Favera, R. (2003). Molecular pathogenesis of non-Hodgkin's lymphoma: the role of Bcl-6. Leuk. Lymphoma *44* (*Suppl 3*), S5–S12.

Peeters, H., and Devriendt, K. (2006). Human laterality disorders. Eur. J. Med. Genet. *49*, 349–362.

Peng, H.B. (1991). *Xenopus laevis*: practical uses in cell and molecular biology. Solutions and protocols. Methods Cell Biol. *36*, 657–662.

Pennekamp, P., Karcher, C., Fischer, A., Schweickert, A., Skryabin, B., Horst, J., Blum, M., and Dworniczak, B. (2002). The ion channel polycystin-2 is required for left-right axis determination in mice. Curr. Biol. *12*, 938–943.

Phan, R.T., and Dalla-Favera, R. (2004). The BCL6 proto-oncogene suppresses p53 expression in germinal-centre B cells. Nature *432*, 635–639.

Ranuncolo, S.M., Polo, J.M., Dierov, J., Singer, M., Kuo, T., Greally, J., Green, R., Carroll, M., and Melnick, A. (2007). Bcl-6 mediates the germinal center B cell phenotype and lymphomagenesis through transcriptional repression of the DNA-damage sensor ATR. Nat. Immunol. *8*, 705–714.

Raya, A., and Belmonte, J.C. (2006). Left-right asymmetry in the vertebrate embryo: from early information to higher-level integration. Nat. Rev. Genet. *7*, 283–293.

Raya, A., Kawakami, Y., Rodriguez-Esteban, C., Buscher, D., Koth, C.M., Itoh, T., Morita, M., Raya, R.M., Dubova, I., Bessa, J.G., et al. (2003). Notch activity

induces Nodal expression and mediates the establishment of left-right asymmetry in vertebrate embryos. Genes Dev. *17*, 1213–1218.

Raya, A., Kawakami, Y., Rodriguez-Esteban, C., Ibanes, M., Rasskin-Gutman, D., Rodriguez-Leon, J., Buscher, D., Feijo, J.A., and Izpisua Belmonte, J.C. (2004). Notch activity acts as a sensor for extracellular calcium during vertebrate left-right determination. Nature *427*, 121–128.

Rones, M.S., McLaughlin, K.A., Raffin, M., and Mercola, M. (2000). Serrate and Notch specify cell fates in the heart field by suppressing cardiomyogenesis. Development *127*, 3865–3876.

Sachs, L.M., and Shi, Y.B. (2000). Targeted chromatin binding and histone acetylation in vivo by thyroid hormone receptor during amphibian development. Proc. Natl. Acad. Sci. USA *97*, 13138–13143.

Schweickert, A., Campione, M., Steinbeisser, H., and Blum, M. (2000). Pitx2 isoforms: involvement of Pitx2c but not Pitx2a or Pitx2b in vertebrate left-right asymmetry. Mech. Dev. *90*, 41–51.

Schweickert, A., Weber, T., Beyer, T., Vick, P., Bogusch, S., Feistel, K., and Blum, M. (2007). Cilia-driven leftward flow determines laterality in *Xenopus*. Curr. Biol. *17*, 60–66.

Shaffer, A.L., Rosenwald, A., Hurt, E.M., Giltnane, J.M., Lam, L.T., Pickeral, O.K., and Staudt, L.M. (2001). Signatures of the immune response. Immunity *15*, 375–385.

Shiratori, H., Sakuma, R., Watanabe, M., Hashiguchi, H., Mochida, K., Sakai, Y., Nishino, J., Saijoh, Y., Whitman, M., and Hamada, H. (2001). Two-step regulation of left-right asymmetric expression of Pitx2: initiation by nodal signaling and maintenance by Nkx2. Mol. Cell *7*, 137–149.

Speder, P., Petzoldt, A., Suzanne, M., and Noselli, S. (2007). Strategies to establish left/right asymmetry in vertebrates and invertebrates. Curr. Opin. Genet. Dev. *17*, 351–358.

Takada, H., Hattori, D., Kitayama, A., Ueno, N., and Taira, M. (2005). Identification of target genes for the *Xenopus* Hes-related protein XHR1, a prepattern factor specifying the midbrain-hindbrain boundary. Dev. Biol. *283*, 253–267.

Tani, S., Kurooka, H., Aoki, T., Hashimoto, N., and Honjo, T. (2001). The N- and C-terminal regions of RBP-J interact with the ankyrin repeats of Notch1 RAMIC to activate transcription. Nucleic Acids Res. *29*, 1373–1380.

Tunyaplin, C., Shaffer, A.L., Angelin-Duclos, C.D., Yu, X., Staudt, L.M., and Calame, K.L. (2004). Direct repression of prdm1 by Bcl-6 inhibits plasmacytic differentiation. J. Immunol. *173*, 1158–1165.

Vasanwala, F.H., Kusam, S., Toney, L.M., and Dent, A.L. (2002). Repression of AP-1 function: a mechanism for the regulation of Blimp-1 expression and B lymphocyte differentiation by the B cell lymphoma-6 protooncogene. J. Immunol. *169*, 1922–1929.

Vonica, A., and Brivanlou, A.H. (2007). The left-right axis is regulated by the interplay of Coco, Xnr1 and derriere in *Xenopus* embryos. Dev. Biol. *303*, 281–294.

Wettstein, D.A., Turner, D.L., and Kintner, C. (1997). The *Xenopus* homolog of Drosophila Suppressor of Hairless mediates Notch signaling during primary neurogenesis. Development *124*, 693–702.

Williams, R., Lendahl, U., and Lardelli, M. (1995). Complementary and combinatorial patterns of Notch gene family expression during early mouse development. Mech. Dev. *53*, 357–368.

Ye, B.H., Lista, F., Lo Coco, F., Knowles, D.M., Offit, K., Chaganti, R.S., and Dalla-Favera, R. (1993). Alterations of a zinc finger-encoding gene, BCL-6, in diffuse large-cell lymphoma. Science *262*, 747–750.

Ye, B.H., Cattoretti, G., Shen, Q., Zhang, J., Hawe, N., de Waard, R., Leung, C., Nouri-Shirazi, M., Orazi, A., Chaganti, R.S., et al. (1997). The BCL-6 proto-oncogene controls germinal-centre formation and Th2-type inflammation. Nat. Genet. *16*, 161–170.

Yoshida, T., Fukuda, T., Hatano, M., Koseki, H., Okabe, S., Ishibashi, K., Kojima, S., Arima, M., Komuro, I., Ishii, G., et al. (1999). The role of Bcl6 in mature cardiac myocytes. Cardiovasc. Res. *42*, 670–679.